A Three-Dimensional Smartphone Positioning Method using a Spinning Magnet Marker

Kosuke Watanabe*, Kei Hiroi†, Takeshi Kamiyama‡, Hiroyuki Sano§, Masakatsu Tsukamoto¶,
Masaji Katagiri§, Daizo Ikeda§, Katsuhiko Kaji‖, Nobuo Kawaguchi†,
*Graduate School of Engineering, Nagoya University
Email: nabeko@ucl.nuee.nagoya-u.ac.jp
†Institutes of Innovation for Future Society, Nagoya University
‡Service Innovation Department, NTT DOCOMO, Inc.
§Research Laboratories, NTT DOCOMO, Inc.
¶Product Department, NTT DOCOMO, Inc.
‖Faculty of Information Science, Aichi Institute of Technology

***Abstract*—We propose a method of detecting the precise three-dimensional position of a smartphone using a Spinning Magnet Marker (SMM). An SMM is a device that generates a dynamic magnetic field by spinning a strong magnet with a motor. In the proposed method, the magnetic sensor of a smartphone detects the magnetic field generated by an SMM, and the three-dimensional position of the smartphone is estimated with an accuracy of better than several tens of centimeters based on the magnetic field and the motor angle of the SMM. It is expected that such precise three-dimensional positioning will enable not only better navigation of users to their destinations but also a better understanding of human behavior. First, we construct theoretical equations relating the magnetic field generated by the SMM to the three-dimensional position of the smartphone in three-dimensional polar coordinates. Second, we evaluate the estimation accuracy of the proposed method with the distance between the SMM and the smartphone fixed at 1.0 m. The azimuth is estimated with a mean error of within 11 degrees, and the elevation is estimated with a mean error of within 10 degrees. The distance is estimated with a mean error of within 19 cm at distances of up to 3.0 m.**

I. INTRODUCTION

Various indoor positioning methods have been studied to date. Methods using microwaves from Wi-Fi access points [1][2] or Bluetooth[3][4] can estimate a position with an error of approximately a few meters, but they are not effective in situations requiring precise location information with errors on the order of a few centimeters. Methods using ultra-wideband (UWB) technology[5] or ultrasound[6] can estimate positions with errors of less than several tens of centimeters, but these methods require a special terminal for position estimation.

In this paper, we propose a three-dimensional smartphone positioning method using a Spinning Magnet Marker (SMM). An SMM generates a dynamic magnetic field by spinning a magnet, and most smartphones include a magnetic sensor, which can detect such a magnetic field. The proposed system can be used to estimate the positions of several smartphones at the same time. We illustrate the concept of our proposal in Fig. 1. Throughout this paper, we denote the distance by "r", the azimuth by "θ", and the elevation by "ψ".

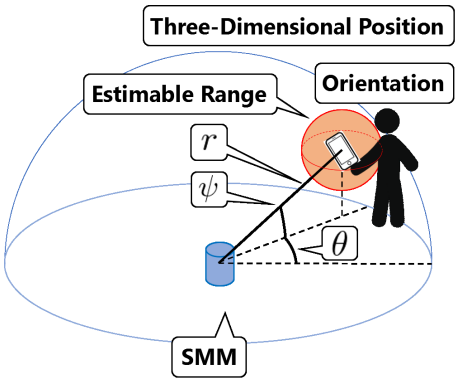

Fig. 1. Concept of positioning using an SMM

There are several advantages to the proposed method. First, this method has higher robustness than that of methods based on radio waves. This is because the magnetic field generated by an SMM is low in frequency and thus has stronger permeability compared with radio waves. In addition, a magnetic sensor can detect the magnetic field from an SMM via frequency analysis even in the presence of an environmental magnetic field. Second, since this method estimates the position of a smartphone, no special terminal is necessary. Third, whereas the other methods mentioned above require at least three devices for position estimation, the proposed method can be applied to estimate a position using only one device.

These advantages enable the precise estimation of the three-dimensional position of a smartphone. As an example of a potential application of this capability, when the precise three-dimensional position of a smartphone near an exhibit at an event venue is known, it can be used to estimate aspects of human behavior, such as the movement of the hand holding the smartphone, and it may also be possible to estimate the flow of people watching the exhibition.

The proposed method is also subject to some difficulties. First, the magnetic sensor of a smartphone has limited sensitivity compared with a biomagnetic sensor. Second, magnetic

TABLE I
COMPARISON WITH PREVIOUS RESEARCHES USING AN SMM

	Estimation Item	Estimable Azimuth	Limit of Estimable Distance[m]
Previous Research (References[8][9])	Detect Passengers, Position (Two-Dimension)	8 Direction	2.0
This Research	Position (Three-Dimension)	100 Direction	3.0

fields are affected by metal, which may affect the estimation accuracy. Previously, we have studied methods of detecting passengers[8] and two-dimensional positioning[9] using an SMM. Table I shows a comparison with our previous research[8][9]. We have achieved improvements over our previous research in the following three respects. First, it is now possible to detect the three-dimensional position of a smartphone. Second, we have developed a new SMM with a step angle of 3.6 degrees, which makes it possible to estimate the azimuth with a resolution of 100 discrete directions. Third, we have improved the estimation accuracy and expanded the estimation range to 3.0 m by adding a procedure for reducing the influence of noise in the magnetic data.

We have estimated the azimuth θ, elevation ψ, and distance r individually to evaluate the corresponding estimation accuracies. In this paper, we explain the methods of estimating the azimuth θ, elevation ψ, and distance r and, finally, the procedure for improving the estimation accuracy.

II. RELATED WORKS

Several positioning methods based on magnetic fields have been proposed to date. In our previous research, Murata et al. studied an indoor positioning method[7] using the residual magnetic field in a building. In this method, the residual magnetic field in a building is measured in advance to create a fingerprint, which is then used to estimate the indoor position. However, this method has the problem that the estimation accuracy greatly depends on the environment.

In addition, POLHEMUS, manufactured by the Polhemus Corporation, is a three-dimensional positioning system that uses magnetic fields. This system enables real-time positioning applications such as motion capture, in which the subject wears one or more sensors that sense a magnetic field generated by a dedicated device. However, because it is necessary to wear special equipment on the arms and waist, this method is considered ineffective for cases in which it is necessary to estimate the positions of many people. Schlageter et al. studied a method of determining the three-dimensional position of a magnet using a two-dimensional arrangement [10]. In this method, the magnetic field generated by the magnet is detected by Hall sensors and used to estimated the magnet's three-dimensional position. Since the target magnet itself generates the magnetic field, this method is low in cost. However, it is difficult to distinguish the magnetic field generated by a target magnet in an environment that contains an ambient magnetic field, such as the geomagnetic field, and the estimation range is limited.

Paperno et al. studied a positioning method [11] using a dynamic magnetic field generated by producing a current flow in a rotating coil. Similarly, Hu et al. studied a positioning method [12] using a dynamic magnetic field generated by three orthogonal coils. In this method, a magnetic sensor detects the dynamic magnetic field at three different frequencies of several kHz, and the signals are used to estimate the three-dimensional position of the magnetic sensor. Since these methods use a dynamic magnetic field, positioning should be possible even in the presence of an environmental magnetic field. However, to continue generating a magnetic field that is detectable by a magnetic sensor at a distance of several meters from the coils, it is necessary to keep a large current flowing, which is problematic in terms of maintenance costs. In addition, since the sampling frequency of a smartphone is approximately several tens of Hz to 100 Hz, the sampling theorem dictates that it is impossible for a smartphone to accurately measure the magnetic field.

Pirkl et al. studied a positioning method [13] based on a low-frequency magnetic field. This method uses transmitter coils to generate a low-frequency magnetic field, which enables the estimation of the three-dimensional position of a receiver composed of coils with an accuracy of better than 1 m^2. Pirkl et al. also studied a proximity detection method for a smartphone and smartwatch [14] using a low-frequency magnetic field. In this method, rectangular 40 cm $\times$ 30 cm coils with 20 windings are placed in a room and used to detect the proximity of a smartphone and smartwatch within a range of 30 cm to 50 cm from the coils. These methods use low-frequency magnetic fields. The first method enables the precise estimation of a three-dimensional position with an accuracy of better than several tens of centimeters, but it requires a special receiver device. The second method uses a smartphone and smartwatch but only permits detection within a close proximity of the coils.

These related works demonstrate that to estimate the position of a smartphone, it is necessary to use a magnetic field oscillating at a low-frequency and to apply a low-cost method of generating the magnetic field.

III. A THREE-DIMENSIONAL SMARTPHONE POSITIONING METHOD

The magnetic sensor in a smartphone can measure the x-, y-, and z-axis components of a magnetic field, and their values are related to the three-dimensional position and orientation of the smartphone. Therefore, it should be possible to estimate the three-dimensional position and orientation of the smartphone based on a magnetic field generated by an SMM.

In this section, we first derive theoretical equations for the magnetic field generated by an SMM in three-dimensional coordinates. Next, we study a method of determining the three-dimensional position of a smartphone from the magnetic field and the motor angle of the SMM.

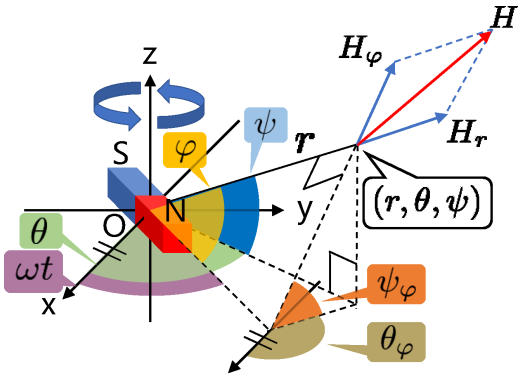

Fig. 2. Magnetic field generated by an SMM

A. Magnetic Field Generated by an SMM

We define the magnetic vectors in a three-dimensional polar coordinate system, as shown in Fig. 2, and use ω to denote the rotation speed of the motor and t to denote time. We assume that the magnetic field generated by a magnet can be approximated as a magnetic field generated by a magnetic dipole. For simplicity, we consider only the case of an azimuth of $\theta = 0$. The magnetic field equations can be written as follows:

$$H_x = H_r \cos\varphi \cos\psi + H_\varphi \sin\varphi \cos\psi_\varphi \cos\theta_\varphi \tag{1}$$

$$H_y = H_\varphi \sin\varphi \cos\psi_\varphi \sin\theta_\varphi \tag{2}$$

$$H_z = H_r \cos\varphi \sin\psi + H_\varphi \sin\varphi \sin\psi_\varphi \tag{3}$$

Next, from Fig. 2, we can derive the relationships between φ, θ_φ, ψ_φ and the azimuth θ, the elevation ψ, and the rotation angle ωt of the motor:

$$\cos\varphi = \cos\psi \cos\omega t \tag{4}$$

$$\cos\theta_\tau = \sin\omega t \frac{\cos^2\psi \sin\omega t \cos\omega t}{\sqrt{1-\cos^2\psi\cos^2\omega t(1+\sin^2\psi)}} \tag{5}$$

$$- \cos\omega t \sqrt{1 - \frac{\cos^4\psi \sin^2\omega t \cos^2\omega t}{1-\cos^2\psi\cos^2\omega t(1+\sin^2\psi)}} \tag{6}$$

$$\cos\psi_\varphi = \sqrt{\frac{1-\cos^2\psi\cos^2\omega t(1+\sin^2\psi)}{1-\cos^2\psi\cos^2\omega t}} \tag{7}$$

The relationships between the azimuth θ and the magnetic field and between the elevation ψ and the magnetic field can be derived using these equations.

B. Azimuth Estimation

The azimuth θ of a smartphone with respect to an SMM can be estimated from the magnetic norm and motor angle. The magnetic norm at the smartphone can be written as shown in equation (8) based on equations (1)∼(7).

$$H = \sqrt{H_\varphi^2 + (H_r^2 - H_\varphi^2)\cos^2\psi\cos^2\omega t} \tag{8}$$

This equation indicates that when $\omega t = \theta$, the magnetic norm is at its maximum. In other words, we can estimate the azimuth from the motor angle at which the magnetic norm is maximal. However, as the motor rotates through 1 period, there are two corresponding azimuth angles θ for which the norm is maximal. Thus, there is a problem of degeneracy, leading to two estimates of the azimuth θ.

C. Elevation Estimation

The elevation ψ of the smartphone with respect to the SMM can be estimated from the magnetic field components in orthogonal coordinates, H_x, H_y, and H_z. To this end, it is necessary to estimate the orientation of the smartphone beforehand and transform the smartphone coordinate system to coincide with that of the SMM; however, we will not discuss this transformation procedure at this time. Equations (9) and (11) can be derived by substituting $\omega t = 0$ into equations (4), (5) and (7) and substituting the resulting equations into equations (1) and (3). Equation (10) can be derived by substituting $\omega t = \pi/2$ into equations (4), (5) and (7) and substituting the resulting equations into equation (2).

$$H_x = -H_\varphi + (H_r + H_\varphi)\cos^2\psi \tag{9}$$

$$H_y = H_\varphi \tag{10}$$

$$H_z = (H_r + H_\varphi)\cos\psi\sqrt{1-\cos^2\psi} \tag{11}$$

Finally, the following equation can be derived by solving equations (9), (10) and (11) for the elevation ψ:

$$\psi = \arccos\left(\frac{H_x + H_y}{\sqrt{(H_x+H_y)^2 + H_z^2}}\right) \tag{12}$$

H_x and H_z are maximal when $\omega t = \theta$. H_y is maximal when $\omega = \theta + \pi/2$. We can estimate the elevation by substituting the amplitude of each magnetic field component into equation (12).

However, unlike for the norm-based estimation of the azimuth θ, since the orthogonal components H_x, H_y and H_z of the magnetic field depend on the orientation of the smartphone, it is necessary to first determine the orientation of the smartphone.

D. Distance Estimation

The distance of the smartphone from the SMM can be estimated from the magnetic norm, which depends on the distance from the SMM. The magnetic field generated by a magnet can be approximated as a magnetic dipole field; therefore, we assume that the magnetic field generated by the magnet along its central axis is inversely proportional to the distance. To investigate the difference in estimation accuracy obtained using different approximation curves, we derive two approximation curves with the forms shown in equations (13) and (14). In these equations, A, B and C are fitting parameters.

$$h_{norm} = Ad^{-B} + C \tag{13}$$

$$h_{norm} = Ad^{-B} \tag{14}$$

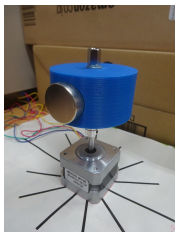

Fig. 3. Spinning magnet marker

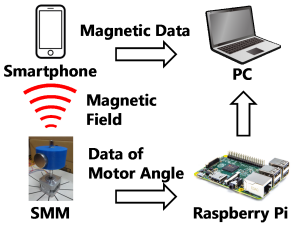

Fig. 4. System configration

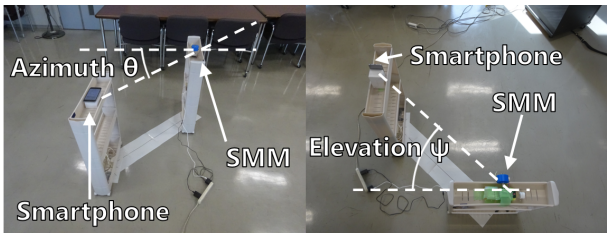

Fig. 5. Experiment situation, left:azimuth, right:elevation

IV. EVALUATION METHOD

A. Design of the SMM

We developed a new SMM design for use in the evaluation experiment. Fig. 3 shows the SMM that was built for this experiment. In our previous study, we could estimate the azimuth θ with a resolution of eight discrete directions[9]. To improve the estimation accuracy, in this study, we used a stepper motor (MERCURY MOTOR SM-42BYG011-25) to spin the magnet. With this stepper motor, the angular data of the motor could be used to estimate the azimuth θ with a resolution of 100 discrete directions thanks to the motor's step angle of 3.6 degrees. We mounted the magnet on a rotating shaft using a mount fabricated using a 3D printer.

Fig. 4 shows the system configuration used in the experiment. The times recorded by the smartphone and the Raspberry Pi were synchronized using NTP (Network Time Protocol). If these times were not synchronized, the accuracy of the azimuth estimation would be greatly affected.

B. Common Experimental Settings

The smartphone used in the experiment was an iPhone 6 Plus, and the sampling frequency of the magnetic sensor was 100 Hz. The rotation speed of the motor was 1 Hz, and the rotation was started from a position corresponding to an azimuth angle of $\theta = 0$ degrees. In this experiment, we fixed the orientation of the smartphone to match the coordinate system of the SMM. Fig. 4 also shows the coordinate system of the smartphone during the experiment.

C. Magnetic Data Processing

Here, we present a procedure for reducing the influence of noise in the measured magnetic data. As the distance from the SMM increases, the influence of noise becomes stronger than the influence of the magnetic field generated by the SMM, and it becomes difficult to distinguish the magnetic field generated by the SMM in the magnetic data. In this section, we describe the processing applied to the magnetic data, and as an example of this processing, we present a case of x-component magnetic data measured at an azimuth of $\theta = 0$ degrees and a distance of 2.0 m from the SMM.

1) Noise Reduction: If we assume that the noise contained in the magnetic data is random, we expect that the influence of the noise can be reduced by averaging the magnetic data. First, we select a data segment corresponding to a measurement time of 10 seconds from the measured magnetic data, and we divide these data into 10 1-second intervals, corresponding to the rotation period of the motor. Then, the times associated with these ten data intervals are re-set to 0 to 1 seconds, and the data are averaged.

Fig. 6 shows the original magnetic data and the magnetic data after processing. From this figure, we can see that the overall trend of the magnetic data is clearer after processing. In addition, when the rotation angle of the motor is 0 degrees, the x-axis component of the magnetic data is maximized. This corresponds to the case in which the azimuth is $\theta = 0$ degrees and the elevation is $\psi = 0$ degrees, and these values are assigned to equation (1) obtained in Section III.

2) Smoothing: Although the influence of noise is reduced by the processing described above, some of this influence still remains. Therefore, we also apply a moving average procedure to the magnetic data as an additional processing step. To achieve appropriate smoothing, we calculated several moving averages with different window widths and different numbers of iterations and compared the results.

Fig. 7 shows the results obtained using several window widths with the number of iterations fixed to 5. In addition, for visual clarity, the vertical scale is changed to 6. Although the smoothing is insufficient with a window width of 2 samples, effective smoothing is achieved with a window width of 3 samples, and the results show no noticeable change with a window width greater than 3 samples. From these observations, we can determine that a window width of 3 samples is sufficient for the smoothing process.

Next, Fig. 8 shows the results obtained by fixing the window width to 3 samples and varying the number of iterations of the moving average procedure. The smoothing does not appear to be sufficient when the number of iterations is 5, but no further noticeable change occurs after 10 iterations. From these findings, we can determine that 10 iterations of the moving average procedure is sufficient.

Based on the above results, we smooth the magnetic data using a window width of 3 samples and 10 iterations of the moving average procedure.

3) Curve Fitting: Approximation curves for each component of the magnetic data can be derived through curve fitting of the data obtained after the previously described processing. As discussed in Section III, we perform sinusoidal curve fitting, using the functional form defined in equation (15), on the magnetic field strength data measured by the magnetic sensor. In addition, we assume that the rotation speed of the SMM is already known to be 1 Hz. In the equation below, h is

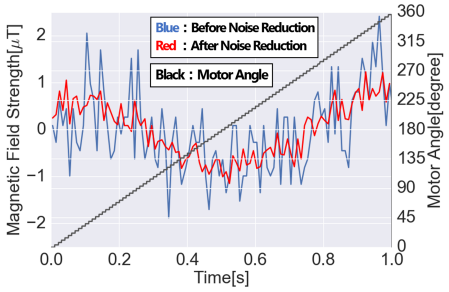

Fig. 6. Before noise reduction and after

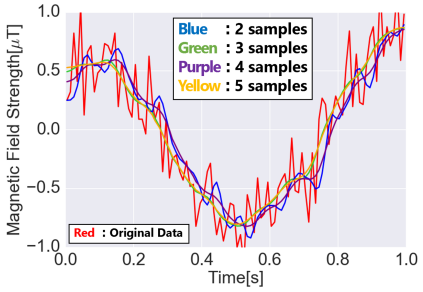

Fig. 7. Comparison with window widths

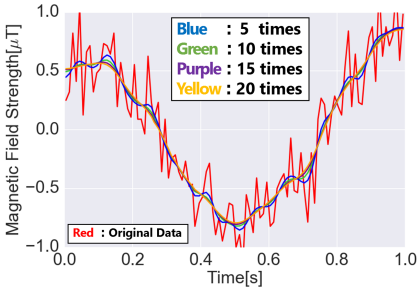

Fig. 8. Comparison with numbers of iterations

the magnetic field value and D, E and F are fitting parameters.

$$h = D\sin(2\pi(\omega t + E)) + F \tag{15}$$

The procedure described above is applied to the magnetic data for each component corresponding to the x, y, and z axes, and the azimuth θ, the elevation ψ, and the distance r are then estimated from these three approximation curves.

V. EVALUATION EXPERIMENT

A. Evaluation of Azimuth Estimation

We fixed the distance between the smartphone and the SMM to 1 m and performed measurements at 8 azimuthal positions of $\theta = 0$, 45, 90, 135, 180, 225, 270 and 315 degrees. Fig. 5 shows the experiment situation. The measurement time was 15 seconds, and estimation was performed 10 times at each position. Table II shows the results. The estimation results presented in this table are rounded off to the nearest whole number. As mentioned in Section II, the proposed method estimates two values of the azimuth θ. We denote these two azimuth estimates by θ'_1 and θ'_2. The mean error was obtained by taking the absolute value of the difference between the true azimuth value and the average of the 10 azimuth estimates.

Next, to study the relationship between the estimation accuracy and the distance from the SMM, we fixed the true azimuth θ and the elevation ψ to 0 and estimated the azimuth θ at 8 locations ranging from 50 cm to 4.0 m from the SMM in intervals of 50 cm. The measurement time was 15 seconds, and estimation was performed 10 times at each location. Fig. 9 shows the results. The estimation results presented in this figure are rounded off to the nearest whole number. The estimation results at distances of up to 3.0 m have a maximum mean error of less than 14 degrees and a standard deviation of less than 12 degrees. By contrast, for the measurements at 3.5 m and 4.0 m, although the mean error is less than 11 degrees, the standard deviation exceeds 30 degrees, indicating that the stability of the estimation is decreasing.

B. Evaluation of Elevation Estimation

It is difficult to estimate a wide range of elevations ψ while remaining at a constant distance. Therefore, in this experiment, we estimated different elevations ψ by turning the SMM and the smartphone sideways in the same direction and then varying the lateral position of the smartphone relative to the SMM. Fig. 5 shows the experiment situation. We fixed the distance from the smartphone to the SMM to 1 m and performed measurements at 5 locations separated by intervals of 30 degrees. The measurement time was 15 seconds, and estimation was performed 10 times at each location. Since two azimuths are estimated, two elevations are also estimated. We denote the two estimated elevations by ψ'_1 and ψ'_2. In addition, we experimented with transforming the smartphone coordinate system to coincide with the SMM coordinate system.

TABLE II
RESULT OF ESTIMATED AN AZIMUTH θ

Azimuth [degree]	0		45		90		135		180	
	θ'_1	θ'_2	θ'_1	θ'_2	θ'_1	θ'_2	θ'_1	θ'_2	θ'_1	θ'_2
Mean Error [degree]	10	9	11	10	1	4	6	3	4	2
Standard Deviation [degree]	5	3	3	3	5	5	6	3	6	6

Table III shows the estimation results rounded off to the nearest whole number. The mean error of the elevation estimates is no more than 10 degrees; thus, the estimation accuracy for the elevation can be considered nearly identical to that for the azimuth. The standard deviation of the elevation estimates is no more than 2 degrees except for an elevation of -60 degrees; this standard deviation is lower than that of the azimuth estimates. This difference is attributed to the smaller effect of the rotation stability of the motor on the elevation estimation compared with the estimation of the azimuth θ, which depends on the motor angle ωt. In addition, the increase in the standard deviation only at an elevation of -60 degrees is considered to be an effect of turning the SMM sideways. Fig. 10 shows the magnetic data measured while estimating the elevations. From this figure, we can see that the magnetic field vectors generated by the SMM form a shape close to an ellipse around the smartphone. As the elevation ψ increases, this ellipse becomes tilted, and it is nearly vertical at an elevation of $\psi = 60$ degrees.

C. Evaluation of Distance Estimation

To estimate the distance of the smartphone from the SMM, we first need to investigate the relationship between the amplitude of the magnetic norm and the distance from the SMM. To do this, we measured the magnetic field at various distances from the SMM in increments of 10 cm. We fixed the azimuth to $\theta = 0$ and the elevation to $\psi = 0$, and the measurement

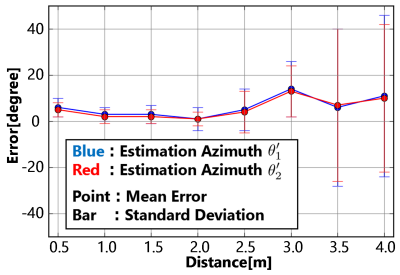

Fig. 9. Accuracy of an estimated azimuth θ

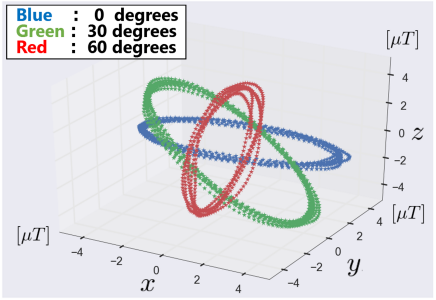

Fig. 10. Magnetic data at each elevation ψ

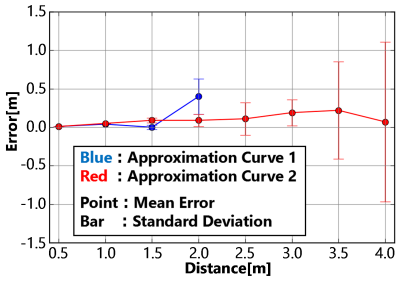

Fig. 11. Accuracy of a estimated distance r

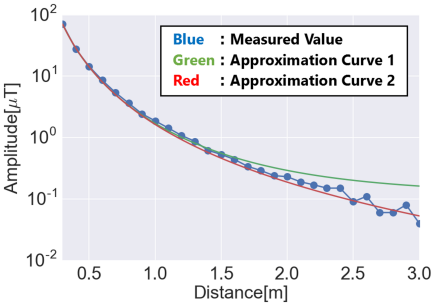

Fig. 12. Norm amplitude （0.3 m∼3.0 m）

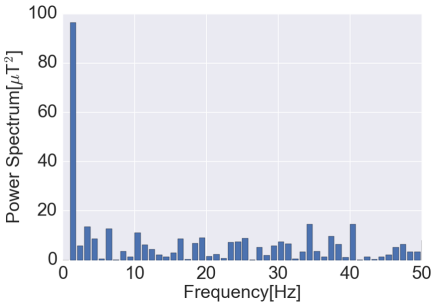

Fig. 13. x-axis power spectrum at 3.0 m

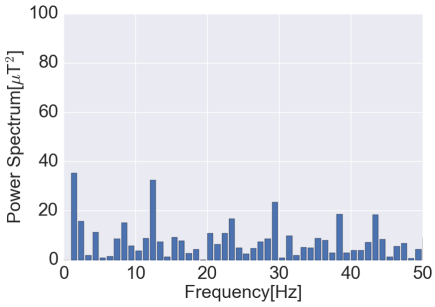

Fig. 14. x-axis power spectrum at 3.5 m

TABLE III
RESULT OF ESTIMATED AN ELEVATION ψ

Elevation [degree]	-60		-30		0		30		60	
	ψ'_1	ψ'_2	ψ'_1	ψ'_2	ψ'_1	ψ'_2	ψ'_1	ψ'_2	ψ'_1	ψ'_2
Mean Error [degree]	8	10	5	2	4	3	3	4	0	4
Standard Deviation [degree]	10	2	2	2	1	1	1	1	2	2

time was 15 seconds. We applied the processing described in Section III to the magnetic data obtained in this experiment to obtain approximation curves describing the behavior of the magnetic norm over time. We subtracted the minimum value from the maximum value of each approximation curve and divided the result by 2 to obtain the norm amplitude. We derived the approximation curves by applying curve fitting to 38 data segments using equations (13) and (14) presented in Section II. We refer to equation (13) as approximation curve 1 and to equation (14) as approximation curve 2. The curve fitting yielded parameters of $A = 1.590$, $B = 3.146$ and $C = 0.111$ for approximation curve 1 and parameters of $A = 1.636$ and $B = 3.124$ for approximation curve 2. These two approximation curves can both be considered to provide reasonable approximations of the magnetic field, as indicated by the decision coefficients of 0.9997 for curve fit 1 and 0.9996 for curve fit 2. Fig. 12 present the curve fitting results.

We then estimated the distance from the smartphone to the SMM using the derived approximation curves. We estimated the distance at 8 locations at distances ranging from 50 cm to 4 m in increments of 50 cm. The measurement time was 15 seconds, and estimation was performed 10 times at each location. Fig. 11 shows the estimation results, which are rounded off to the nearest third decimal place. The results obtained using approximation curve 1 are higher in accuracy than those obtained using approximation curve 2 for distances of up to 1.5 m; however, distances greater than 2.5 m could not be successfully estimated using approximation curve 1. The reason for this, as shown in Fig. 12, is that approximation curve 1 begins to deviate from the measured data at distances greater than 1.0 m. In addition, when the norm amplitude is smaller than $C = 0.111$, distance estimation using this curve becomes impossible because there is no corresponding distance value. By contrast, the accuracy of the estimation results obtained using approximation curve 2 is higher than that for approximation curve 1 at distances greater than 2.0 m, and it is possible to estimate distances of more than 2.5 m using approximation curve 2. Up to a distance of 3.0 m, the mean error is no more than 19 cm, and the standard deviation is 17 cm. At distances of 3.0 m and 3.5 m, the mean errors are no more than 22 cm; however, the standard deviations are more than 50 cm and 1.0 m, respectively, at these distances. These findings indicate that the stability of the estimation decreases as the distance increases. Table IV presents a comparison with our previous research [9]; the results indicate improvement compared with our previous study.

Finally, we investigated the greatest distance at which the magnetic sensor could detect the magnetic field generated by the SMM. Fig. 13 and 14 show the power spectrum of the x-axis component of the magnetic field at distances of 3.0 m and 3.5 m, respectively. In the power spectrum corresponding to 3.0 m, a peak appears at 1 Hz, which is the rotation speed of the motor. However, at 3.5 m, the peak at 1 Hz

TABLE IV
MEAN ERROR OF ESTIMATED DISTANCE r COMPARED WITH PREVIOUS RESEARCH

	$\sim$1.4 m	$\sim$2.0 m	$\sim$3.0 m
Previous Research (References[9])	4 cm	13 cm	No Data
This Research	$\leq$1 cm	9 cm	19 cm

is of approximately the same strength as the noise, and it becomes difficult for the smartphone to detect the magnetic field generated by the SMM. The reason why the standard deviation of the estimates increases as the distance increases is that the influence of noise can no longer be sufficiently reduced by the method presented in Section III.

VI. CONCLUSION

In this study, we investigated a three-dimensional positioning method for a smartphone using an SMM. At a distance of 1 m from the SMM, the azimuth could be estimated with a mean error of within 11 degrees and a standard deviation of within 6 degrees, and the elevation could be estimated with a mean error of within 10 degrees and a standard deviation of within 10 degrees. Next, we conducted an experiment to evaluate the relationship between the distance from the SMM and the estimation accuracy. At distances ranging from 0.5 m to 4.0 m in increments of 0.5 m, we could estimate the distance with a mean error of within 19 cm and a standard deviation of within 21 cm and could estimate the azimuth with a mean error of within 14 degrees and a standard deviation of within 12 degrees.

As a future task, it is necessary to estimate the distance r, the azimuth θ, and the elevation ψ at the same time and evaluate the estimation accuracy. In addition, in this study, we conducted our experiments with a stationary smartphone. In the future, it will be necessary to consider a method of estimating the trajectory of a moving smartphone. Furthermore, although we considered only three-dimensional positioning in this paper, we plan to also consider the estimation of the smartphone orientation in the future. The degeneracy problem that results in two azimuth estimates is also expected to be solved, and a method of estimating the elevation even at an arbitrary orientation should be investigated as well.

ACKNOWLEDGEMENT

This work was supported by JSPS KAKENHI Grant Number JP17H01762.

REFERENCES

[1] Kaji, K., Kawaguchi, N., Design and Implementation of WiFi Indoor Localization based on Gaussian Mixture Model and Particle Filter, Proceedings of the International Conference on Indoor Positioning and Indoor Navigation (IPIN'12), pp.89-92, 2012.

[2] Zhuang, Y., Syed, Z., Georgy, J., El-Sheimy, N., Autonomous smartphone-based WiFi positioning system by using access points localization and crowdsourcing, Pervasive and Mobile Computing, Vol.18, pp.118-136, 2015.

[3] Oksar, I., A Bluetooth Signal Strength Based Indoor Localization Method, In Proceedings of 2014 Internatinal Conference on Systems, Signals and Image Processing(IWSSIP), pp.251-254, 2014.

[4] Rida, M., Liu, F., Jadi, Y., Algawhali, A., Askourih, A., Indoor Location Position Based on Bluetooth Signal Strength, In Proceedings of the 2nd International Conference on Information Science and Control Engineering, pp.769-773, 2015.

[5] Muller, P., Wymeersch, H., Piche, R., UWB Positioning with Generalized Gaussian Mixture Filters, Mobile Computing, IEEE Transactions on, Vol.13, Issue10, pp.2406-2414, 2014.

[6] Medina, C., Segura, J., Angel, D., Ultrasound Indoor Positioning System Based on a Low-Power Wireless Sensor Network Providing Sub-Centimeter Accuracy, Sensors (Switzerland), Vol.13, Issue.3, pp.3501-3526, 2013.

[7] Murata, Y., Kaji, K., Hiroi, K., Kawaguchi, N., Pedestrian Dead Reckoning based on Human Activity Sensing Knowledge, In Proceedings of the 2nd International Workshop on Human Activity Sensing Corpus and its Application (HASCA2014), pp.797-806, 2014.

[8] Takeshima, T., Kaji, K., Hiroi, K., Kawaguchi, N., Kamiyama, T., Ota, K., Inamura, H., A Pedestrian Passage Detection Method by Using Spinning Magnets on Corridors, Journal of Information Processing Society of Japan, Vol.58, No.1, 2017.

[9] Takeshima, T., Kaji, K., Hiroi, K., Kawaguchi, N., Kamiyama, T., Ota, K., Inamura, H., A Three-Dimensional Smartphone Positioning Method Based on Spinning Magnet Marker, Multimedia, Distributed, Cooperative, and Mobile Symposium（DICOMO2016）, Vol.2016, pp.889-898, 2016.

[10] Schlageter, V., Drljaca, P., Popovic, R., Kucera, P., A Magnetic Tracking System based on Highly Sensitive Integrated Hall sensors, JSME International Journal Series C, Vol.45, Issue.4, pp.967-973, 2002.

[11] Paperno, E., Sasada, I., Leonovich, E., A New Method for Magnetic Position and Orientation Tracking, IEEE Transactions on Magnetics, Vol.37, Issue.41, pp.1938-1940, 2001.

[12] Hu, C., Song, S., Wang, X., Meng, M., Li, B., A Novel Positioning and Orientation System Based on Three-Axis Magnetic Coils, IEEE Transactions on Magnetics, Vol.48, Issue.7, pp.2211-2219, 2012.

[13] Pirkl, G., Lukowicz, P., Robust, Low Cost Indoor Positioning Using Magnetic Resonant Coupling, Ubicomp, pp.431-440, 2012.

[14] Pirkl, G., Hevesi, P., Cheng, J., Lukowicz, P., mBeacon: Accurate, robust proximity detection with smart phones and smart watches using low frequency modulated magnetic fields, Proceedings of the 10th EAI International Conference on Body Area Networks, pp.186-191, 2015.